Development of a Novel Wireless Electric Power Transfer System for Space Applications

Gabriel VAZQUEZ RAMOS
National Aeronautics and Space Administration
Launch Services Program (Mail Code: VA-H3)
John F. Kennedy Space Center, FL 32899
Gabriel.VazquezRamos-1@nasa.gov

and

Dr. Jiann-Shiun YUAN
University of Central Florida
Department of Electrical Engineering and Computer Science
Orlando, FL 32816-2362
yuanj@mail.ucf.edu

ABSTRACT

This paper will introduce a new implementation for wireless electric power transfer systems: space applications. Due to the risks that constitute the use of electrical connector for some space missions/applications, a simple wireless power system design approach will be evaluated as an alternative for the use of electrical connectors. This approach takes into consideration the overall system performance by designing the magnetic resonance elements and by verifying the overall system electrical behavior. System characterization is accomplished by executing circuit and analytical simulations using Matlab® and LTSpiceIV® software packages. The design methodology was validated by two different experiments: frequency consideration (design of three magnetic elements) and a small scale proof-of-concept prototype. Experiment results shows successful wireless power transfer for all the cases studied. The proof-of-concept prototype provided ~4 W of wireless power to the load (light bulb) at a separation of 3 cm from the source. In addition, a resonant circuit was designed and installed to the battery terminals of a handheld radio without batteries, making it turn on at a separation of ~5 cm or less from the source. It was also demonstrated by prototype experimentation that multiple loads can be powered wirelessly at the same time with a single electric power source.

Keywords: Magnetic Resonance, Wireless Power Transfer, Magnetic Coupling, Space Systems, Power Amplifier.

1. INTRODUCTION

For Space Systems, power connectors constitute a vital and complicated component required for the success of every space mission. Some of these missions require crucial connector mate and de-mate operations in environments full of contaminants and/or performed by automatic (unmanned) systems. These operations can constitute a risk to the mission due to connector deterioration after been exposed to environmental contaminates (i.e. lunar regolith, also call moon dust) or by bended pins due to misaligning during a connector mate operation [1]. To mitigate these concerns, this paper is proposing the use of a wireless power transfer (WPT) system for space applications. This will be accomplished by the evaluation and implementation of the magnetic resonance concept for space systems.

In classical physics, mechanical resonance has been widely demonstrated in various applications and experiments (i.e. identical tuning forks resonating by only impacting one). In 2007, a research team from the Massachusetts Institute of Technology demonstrated a similar principle on electric circuits called magnetic resonance (also known as magnetic coupling) [2].

The WPT system proposed in this paper will transfer electric power without the need of having physical electrical connection. The intent is to have a modular design that can be used as a "wireless power connector" in a wide range of space exploration applications (i.e. automatic docking systems for space systems rendezvous, wireless sensors for launch vehicles, wireless battery charging systems, robotic mission charging stations on other planets, moons and asteroids, etc.). The main scope of this paper is to provide a simple design approach for the implementation of a WPT and its feasibility for space applications.

2. ANALYSIS

Based on technical literature review, peer reviewed papers, and component level testing, a simple design approach will be delineated for the analysis and fabrication of WPT devices. A block diagram is provided in Fig. 1, showing the main elements required for the WPT system implementation.

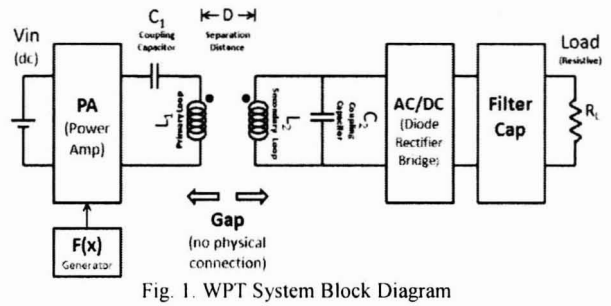

Fig. 1. WPT System Block Diagram

Overall System Operation

An electric source circuit generates a sinusoidal signal (represented by a power amplifier, PA, in Fig. 1) inducing magnetic pulsation signals at the primary loop (L_1) of the source resonating circuit (C_1 and L_1). The secondary loop (L_2) will receive the magnetic pulses due to the fact that is part of the load resonating circuit (C_2 and L_2). The load resonating circuit is tuned to the same frequency as the primary circuit. This magnetic energy induces a sinusoidal electric signal in the secondary [2]. The alternate current (AC) signal is then rectified by a diode H-bridge and a capacitor to provide a direct current (DC) signal to the load. This process will transfer energy wirelessly from the primary circuit (Vin, source) to the secondary circuit (Load) [2].

The overall system analysis and design was performed by a systematic series of simulations using the combination of Matlab® and LTSpiceIV® software packages. This integrated system circuit simulation combines different technical topics evaluated for the design. These topics were divided into two main design simulations: magnetic elements simulation and system circuit simulation. Each of these simulations provides an important contribution for the overall understanding of the system's electrical behavior.

Magnetic Elements Simulation

The magnetic elements (Fig. 2) will be defined as the primary and secondary loops with their respective coupling capacitor for resonant circuit. To determine the magnetic element parameters, a Matlab® based code was generated using simple electromagnetic and circuit equations. This tool helped us to understand how to design the inductor loops and their corresponding coupling capacitor for the desired operating frequency.

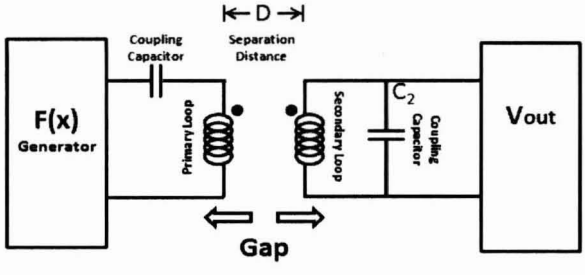

Fig. 2. WPT System Magnetic Element Definition

The Eq. (1) defines the self inductance (L) of an inductor loop with no magnetic core [3].

$$L = N^2 * R * \mu_0 * \left[\ln\left(\frac{8*R}{r}\right) - 1.75\right] \qquad (1)$$

Where:

L = inductance of the loop
N = number of turns in the loop
R = radius of the loop
r = loop conductor radius
μ_0 = permeability of vacuum

In order to adequately transfer power wirelessly, the primary and the secondary magnetic loops need to be tuned to the same resonant frequency (ω_0, f_o). This tuning is accomplished by connecting a capacitor in series to the primary circuit and in parallel to the secondary circuit (also known as series-parallel coupling) [4]. The Eq. (2) is utilized to determine the capacitor value required to generate the resonant circuit with the inductor [5]:

$$C = \frac{1}{\omega_0{}^2 * L} \qquad (2)$$

Where:

C = coupling capacitance required
ω_0= frequency of oscillation [rad/sec]
L = inductance of the coil

An additional important calculation to be considered is the mutual inductance between the two loops. This value will be calculated for the required separation distance of the vacuum gap and then simulated in LTSpiceIV® to determine the overall circuit response. Before calculating the mutual inductance, it is required to determine the magnetic coupling coefficient using the Eq. (3) [6]. By using the magnetic coupling coefficient, a characterization of the mutual inductance can be obtained with Eq. (4) [7].

$$k = \frac{1}{\left[1+2^{2/3}\left(\frac{D}{\sqrt{R1*R2}}\right)^2\right]^{3/2}} \qquad (3)$$

$$L_M = k * \sqrt{L_1 * L_2} \qquad (4)$$

Where:

k= mutual coupling coefficient
D = physical distance between L_1 and L_2
R_1 = radius of the loop 1
R_2= radius of the loop 1
L_M= mutual inductance
L_1 = inductance of the loop 1
L_2 = inductance of the loop 2

A simple proof-of-concept prototype was assembled to demonstrate the proposed design methodology. The parameters used in the proof-of-concept prototype are listed in Table 1. These parameters will be later used to calculate the coupling capacitors, self inductance of the loops, and mutual inductance parameters. The calculated parameters using the developed Matlab® code are shown in Table 2.

Table 1: Proof-of-Concept Prototype Characteristics

Parameter	Symbol	Value	Units
Number of turns	N_1 & N_2	8	turns
Radius of the Loops	R_1 & R_2	0.24	m
Loop conductor radius	r_1 & r_2	0.001	m
Loop conductor resistance (in DC)	a	0.064*	Ohm
Frequency of operation	f_0	15	kHz
	ω_0	94.25	k Rad/s
Vacuum Permeability	μ_0	$4*\pi*10^{-7}$	H/m
Separation distance	D	0.03	m
Load (light bulb)	R_0	4**	Ohms

* The loop conductor resistance (litz wire cable) was calculated using reference [8]
** Measured resistance for the filament. However, it was noted after system simulation and prototype experimentation that the light bulb filament was behaving as a 40 Ohms resistor.

Table 2: Calculated Prototype Circuit Parameters

Parameter	Symbol	Value	Units
Self Inductance	L_1 & L_2	49.38	μH
Mutual Inductance	L_M	42.85	μH
Coupling Capacitor	C_1 & C_2	2.14*	μF
Leakage Inductances	L_{lk1} & L_{lk2}	6.533	μH

* Mylar capacitors of 2.2uF (5% accuracy) were used. After circuit testing, the coupling frequency was found to be 15.5 kHz.

System Circuit Simulation

To characterize the overall circuit performance, it was required to find a circuit model that can help predict the performance of the overall system. The model used to emulate the behavior of the two hollow inductor loops (under magnetic resonance) is the non-ideal transformer equivalent circuit [9]. Fig. 3 illustrates the equivalent circuit of the two loops in magnetic resonance configuration.

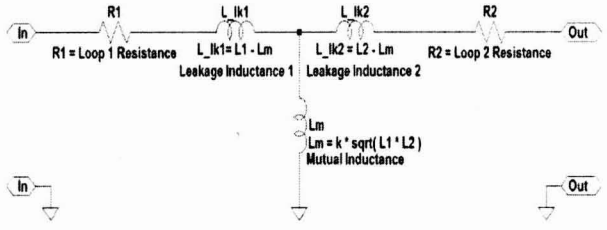

Fig. 3. Equivalent Circuit for Two Hollow Inductors (N1 = N2)

By implementing the non-ideal transformer equivalent circuit, the overall circuit was simulated in LTSpiceIV® using the parameters previously calculated (Table 2). Fig. 4 illustrates the coupling configuration that was simulated as a "series-shunt" coupling [5]. A generic sinusoidal voltage generator was used to simulate the power provided by the PA.

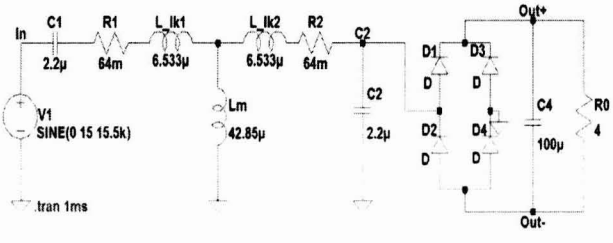

Fig. 4. Wireless Power Transfer Model with Calculated Loop Inductances with a Separation Distance of D = 3 cm

The simulation outputs of the circuits shown in Fig. 4 are illustrated in Fig. 5. The green trace is the function generator/power amplifier voltage source (V_{IN}), the blue trace is the secondary voltage before rectification (V_{C2}) and the red trace is the output voltage ($V_{OUT+, OUT-}$) of the circuit.

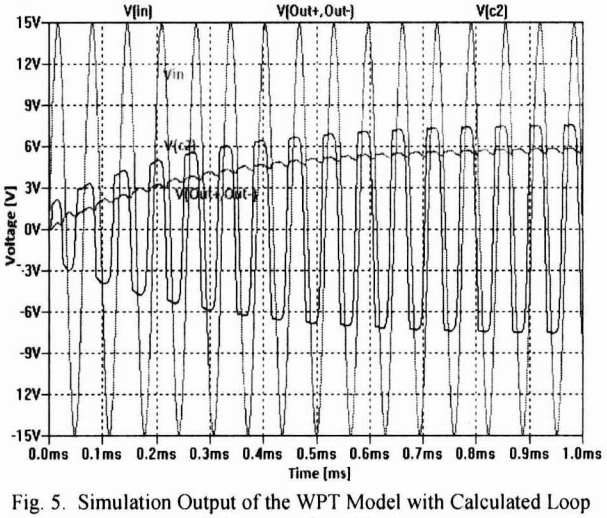

Fig. 5. Simulation Output of the WPT Model with Calculated Loop Inductances from Fig. 4

3. RESULTS

The analysis previously discussed was validated using two different experiments to better characterize the magnetic resonance concept: frequency considerations and a small scale proof-of-concept prototype.

Experiment #1: *Frequency Considerations*

To analyze the frequency of operation effects, three circuit configurations were designed with the same inductor loop characteristics (Table 3). The three frequencies of operation studied were: 84 kHz, 839 kHz and 1.757 MHz. The self inductances of the magnetic loops were determined with the Eq. (1) and coupling capacitors were selected to match the frequency of operation according to the Eq. (2). The testing configuration is illustrated in Fig. 2. The main objective of this test was to preliminary study the magnetic element behavior at different frequencies and validate that magnetic resonance can be achieved with the design approach described in the previous section (*Analysis*).

Table 3: Magnetic Loop Design Characteristics

Characteristic	Loop 1	Loop 2
Radius [cm]	7.5	7.5
Number of Turns	7	7

The frequency consideration test results are listed in Table 4 and illustrated in Fig. 6. The testing circuit (Fig. 2) was powered by a function generator. The settings of the function generator remained unchanged throughout these tests for all three cases. The main objective of this experiment was met (to validate the magnetic coupling design approach described in the *Analysis* section). In addition, it was also noticed for the frequencies studied that magnetic coupling is greater at higher frequencies of operations. Further analysis/testing will be required to determine which frequency is the optimal.

Table 4: Frequency Consideration Test Results

Frequency of Operation	Separation Distance (cm)	Vout (Vpeak)
f_s = 84 kHz	D_1 = 0	5 V
	D_2 = 4	1.5 V
	D_3 = 14	200mV
f_s = 839 kHz	D_1 = 0	10 V
	D_2 = 4	20 V
	D_3 = 14	2.2 V
f_s = 1.757 MHz	D_1 = 0	15 V
	D_2 = 4	34 V
	D_3 = 14	5 V

Note: The settings of the function generator (V_{in}) remained unchanged throughout these tests (all three cases).

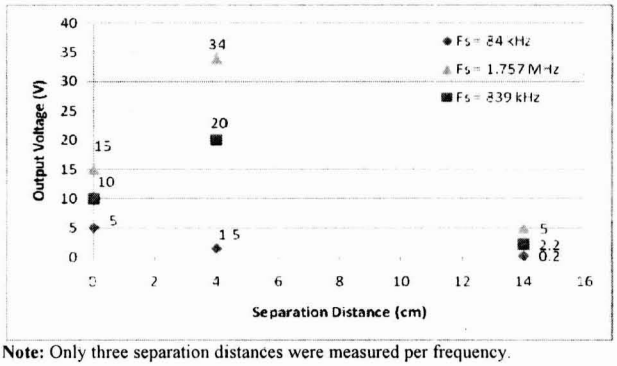

Note: Only three separation distances were measured per frequency.

Fig. 6. Frequency Consideration Test Results

Experiment #2: Small Scale Proof-of-Concept Prototype

A small scale proof-of-concept prototype was assembled with the values provided on Table 1 and Table 2 to validate the design approach discussed in the *Analysis* section. Using the block diagram in Fig. 1 as the design guideline, a series of commercial parts were evaluated, individually tested and selected to complete the prototype design (Fig. 7).

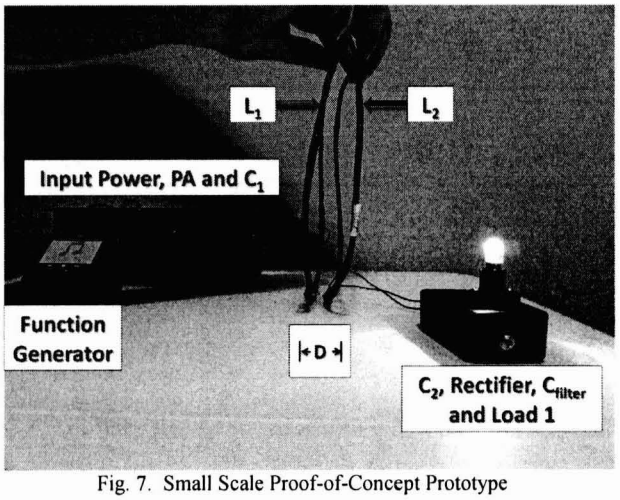

Fig. 7. Small Scale Proof-of-Concept Prototype

Due to the fact that the loops inductors were manually built, variably on the inductance value is expected. The Agilent LCR Meter 4980A was used to measure the inductances of the loops at the prototype operating frequency (15.5 kHz). Table 5 lists the measured loop inductances and the calculated mutual inductance for a separation distance of 3cm. Fig. 8 illustrates the inductors built for the small scale prototype.

Table 5: Measured Loop Inductances and Mutual Inductance

Parameter	Symbol	Value	Units
Self Inductance #1	L_1	44.1	μH
Self Inductance #2	L_2	54.3	μH
Mutual Inductance*	L_M	42.46	μH
Leakage Inductance 1*	L_{lk1}	1.638	μH
Leakage Inductance 2*	L_{lk2}	11.84	μH

* Value calculated based on the measured self inductances (L_1 and L_2) and using a separation distance of 3 cm.

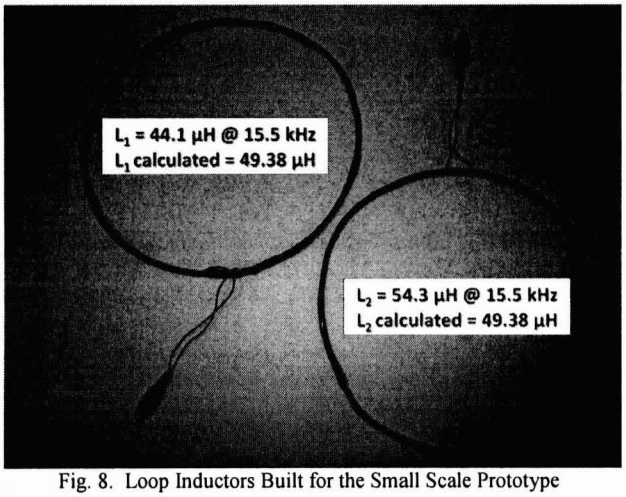

Fig. 8. Loop Inductors Built for the Small Scale Prototype

The WPT LTSpiceIV® model was updated with the loop measurements acquired with the LCR meter (Fig. 9) and the simulation output is illustrated in Fig. 10. The green trace is the function generator/power amplifier voltage source (V_{IN}), the blue trace is the secondary voltage before rectification (V_{C2}) and the red trace is the circuit output voltage ($V_{OUT+, OUT-}$).

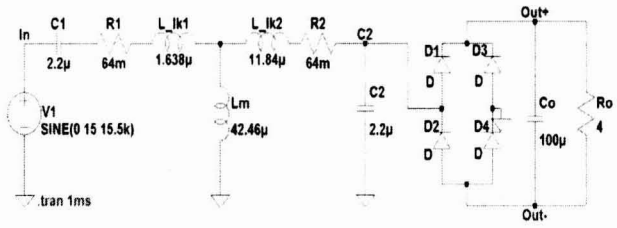

Fig. 9. Wireless Power Transfer Model with Measured Loop Inductances with a Separation Distance of D = 3cm

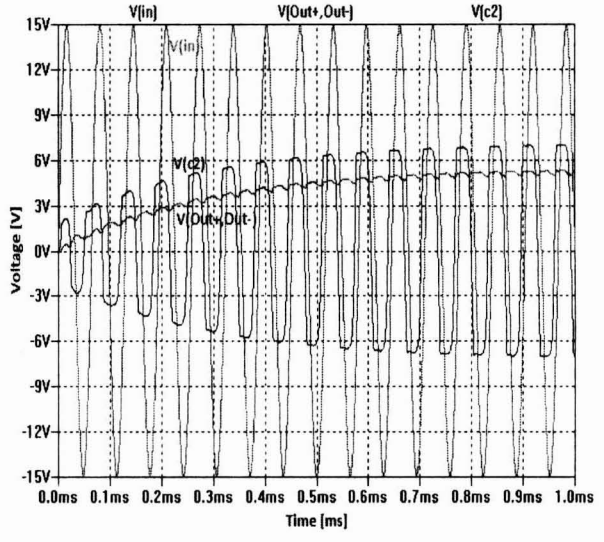

Fig. 10. Simulation Output of the WPT Model with Measured Loop Inductances (Fig. 9)

The system operating frequency (f_0) was targeted to be 15 kHz; however, after further calibration and tuning, the system demonstrated to be magnetically coupled at ~15.5 kHz. This discrepancy is attributed to the coupling capacitor tolerance of 5%, the loop conductor radius measurement and the variability of the manually built inductor loops. An accurate representation of the loop conductor radius and coupling capacitor values are required for an accurate system coupling according to Eq. (1), Eq. (2) and Eq. (3).

Two different alternatives were implemented/designed to provide the frequency of operation (sinusoidal at 15.5 kHz) required by the PA: XR2206 function generator integrated circuit [10] and by programming an audio signal. The audio signal was programmed in Matlab® as a sinewave with the required frequency, an audio file format (Windows Media Audio or WMA) was generated using Matlab®'s "*wavwrite()*" command and then the audio file was downloaded and played using the iPhone music player. The iPhone's output is connected to the PA as the function generator (Fig. 11). The amplitude of this signal was controlled by the volume of the iPhone. Fig. 11 illustrates the output voltage supplied by the iPhone using the audio signal programmed in Matlab®.

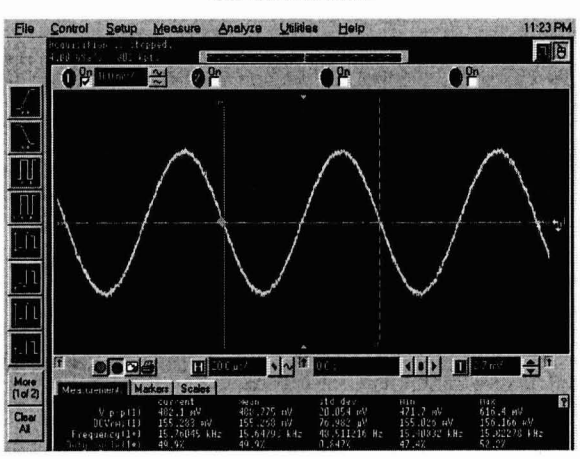

Fig. 11. iPhone Output Used as a Function Generator (PA Input Signal)

The V_{DC} power supply was selected to be the Lexmark z23 printer power adapter (30 Vdc and up to 0.5 Amp). By the use of voltage regulators (LM7809, LM7812 and LM7815), the voltage was stepped down to supply the required voltage to all the electronics subsystems and components used on the prototype. For a simple PA implementation, the frequency of operation was selected to be within audible range (20 Hz- 20 kHz). This enables us to use the "off-the-shelf" commercial PA: Velleman-Kit K4001 [11].

As the WPT system block diagram illustrate in Fig. 1, the PA will supply the required power of the source resonant circuit (C_1 and L_1). The source loop (L_1) voltage will induce the magnetic resonance effect into the load loop (L_2) through the load resonant circuit (C_2 and L_2) [2]. The source and load loops voltages (at $D \approx 0$ cm) are illustrated in Fig. 12 and Fig. 13 respectively.

An AC-to-DC converter (rectifier) was design to transform the received AC signal (at L_2) to the DC signal required by the load. The rectifier was design using 1n5817 Schottky barrier diodes connected on an H-bridge configuration. Schottky barrier diodes where selected due to their fast recovery time. Based on simulation trials, the filter capacitor was selected to be 100μF.

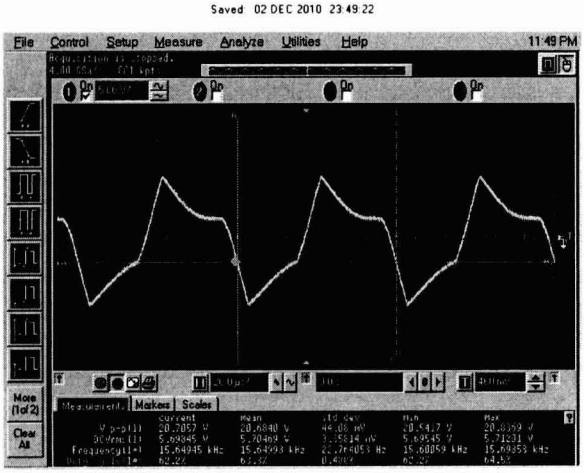

Fig. 12. Source Loop (L_1) Voltage

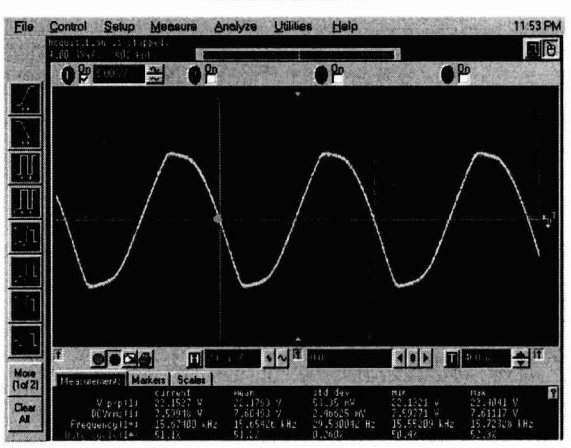

Fig. 13. Voltage Induced at the Load Loop (L_2)

The prototype performance was carefully characterized by measuring and plotting the output root mean square (RMS) voltage, current and power for different source/load separation distances (Fig. 14, Fig. 15 and Fig. 16). It is noticed that the optimum power transfer separation is about 3 cm (~4W). The peak power transfer distance result concurred with a similar study performed on magnetic resonance [12].

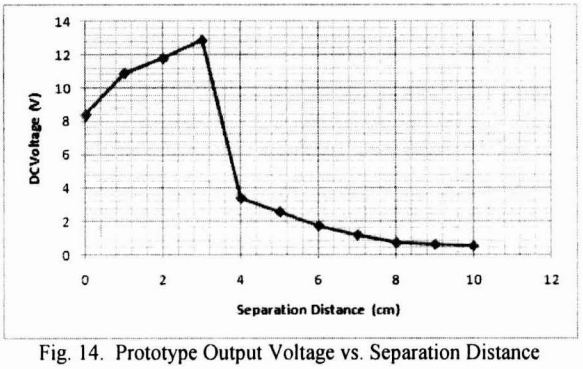

Fig. 14. Prototype Output Voltage vs. Separation Distance

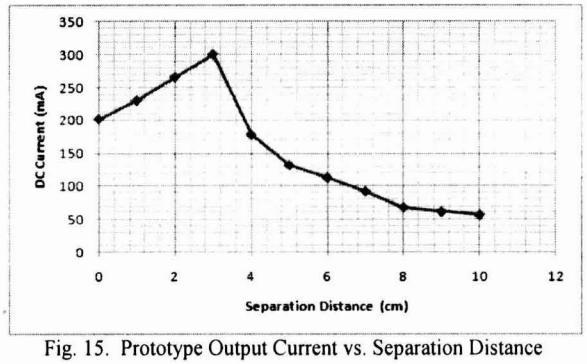

Fig. 15. Prototype Output Current vs. Separation Distance

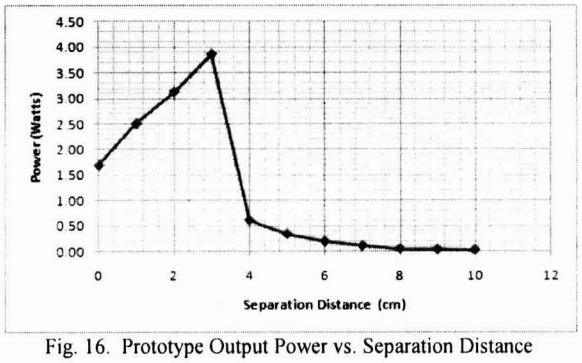

Fig. 16. Prototype Output Power vs. Separation Distance

It is noticed that the theory presented in the *Analysis* section provides similar results than the small scale proof-of-concept prototype experimental results. However, it is also noticed that due to parasitic effects and unwanted capacitive coupling, internal to the inductor windings, provides an unpredicted response in the test data. Further analysis and experimentation will be required for an overall more accurate electrical characterization of the system.

An additional test performed to the prototype was to add a non-conductive material between the source element and the load element (i.e. wood, plastic, etc.). As expected, magnetic coupling was achieved even through a non-conductive material.

A second load was designed to operate using the prototype source (Fig. 17). A receiving magnetic element was designed and connected to the battery terminals of a handheld radio (Durabrand PR-355 AM/FM Sports Radio) to resonate at the same frequency as the wireless power source previously described (f_0 = 15.5kHz). The WPT receiver device designed to the handheld radio replaced the use of 3 AA batteries. The radio turns on within a proximity of ~5 cm from the source. It was also noticed that the radio and the light bulb can receive power wirelessly at the same time using the same power source.

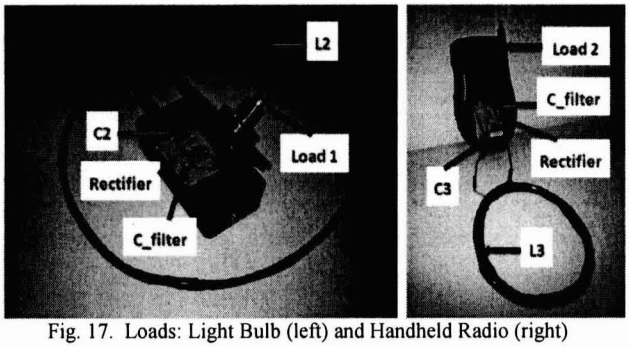

Fig. 17. Loads: Light Bulb (left) and Handheld Radio (right)

4. CONCLUSION

Theory analysis and experimental results suggest that magnetic resonance is a feasible and reliable technology that represents an alternative to conventional electric connectors. Preliminary testing also showed that magnetic resonance can be achieved through non-conductive materials (i.e. wood, plastic, etc.). Multiple mobile devices can be powered/recharged at the same time using a single source. This was accomplished by tuning the source and all the loads to the same operating frequency. In addition, it was demonstrated by prototype experimentation that magnetic resonance can be achieved within audible frequencies ($20Hz \leq f_0 \leq 20$ kHz). This can represent a major industrial advantage due to the fact that there are currently a wide range of options available for audio power amplifiers.

More testing and experimental data will be required for the implementation of a reliable and efficient wireless power system for space applications. In theory, the magnetic resonance principle is believed to operate in the space environment. However, using the principles discussed in this paper and additional analysis, a more advanced design will be evaluated for compliance to NASA and other military systems standards [13][14][15][16]. Design compliance to these standards will be highly dependent on the system application (i.e. launch vehicles, spacecraft, rover, wireless battery charger, docking systems, etc.)

5. BIBLIOGRAPHY

[1] National Aeronautics and Space Administration *Workmanship Problems Pictorial Reference/Wiring and Cabling* **NASA Electric Parts and Packaging Program** (Online) *URL: http://nepp.nasa.gov/index.cfm/14257*

[2] Aristeiidis Karalis, J.D. Joannopoulos, Marin Soljacic. "Efficient Wireless Non-Radiative Mid-Range Energy Transfer", **Annals of Physics**, Vol. 323, 2008, pp. 34-48.

[3] Chunbo Zhu; Kai Liu; Chunlai Yu; Rui Ma; Hexiao Cheng; , "Simulation and experimental analysis on wireless energy transfer based on magnetic resonances," **Vehicle Power and Propulsion Conference, 2008. VPPC '08. IEEE**, 3-5 Sept. 2008, pp.1-4

[4] Stielau, O.H.; Covic, G.A.; "*Design of loosely coupled inductive power transfer systems*," **Power System Technology, 2000. Proceedings. PowerCon 2000. International Conference on**, vol.1, 2000 pp.85-90

[5] Chunbo Zhu; Chunlai Yu; Kai Liu; Rui Ma; "Research on the topology of wireless energy transfer device," **Vehicle Power and Propulsion Conference, 2008. VPPC '08. IEEE** , 3-5 Sept. 2008, pp.1-5

[6] Mur-Miranda, J.O.; Fanti, G.; Yifei Feng; Omanakuttan, K.; Ongie, R.; Setjoadi, A.; Sharpe, N.; , "Wireless power transfer using weakly coupled magnetostatic resonators," **Energy Conversion Congress and Exposition (ECCE), 2010 IEEE** , 12-16 Sept. 2010, pp.4179-4186,

[7] Hee-Seung Kim; Do-Hyun Won; Byung-Jun Jang; , "Simple design method of wireless power transfer system using 13.56MHz loop antennas," **Industrial Electronics (ISIE), 2010 IEEE International Symposium on** , 4-7 July 2010., pp.1058-1063,

[8] New England Wire Technologies **Litz Wire Technical Information 2005** New England Wire Technologies, NH

[9] Judek, S.; Karwowski, K.; , "Supply of electric vehicles via magnetically coupled air coils," **Power Electronics and Motion Control Conference, 2008. EPE-PEMC 2008. 13th** , 1-3 Sept. 2008pp.1497-1504

[10] EXAR Corporation. **XR 2206 Function Generator IC**, EXAR Corporation, 2007.

[11] Velleman Components NV. **7W Mono Amplifier, Kit**. Velleman Components NV. K4001.

[12] Shen, F. Z.; Cui, W. Z.; Ma, W.; Huangfu, J. T.; Ran, L. X.; , "Circuit analysis of wireless power transfer by "coupled magnetic resonance"," **Wireless Mobile and Computing (CCWMC 2009), IET International Communication Conference on** , 7-9 Dec. 2009, pp.602-605

[13] National Aeronautics and Space Administration. **Electrical Bonding for NASA Launch Vehicles, Spacecraft, Payloads, and Flight Equipment**, Washington, D.C., NASA, NASA-Std-4003.

[14] United States Department of Defense. **Requirements of the Control of Electromagnetic Interference Characteristics of Subsystems and Equipment**. Wright-Patterson Air Force Base, OH, United States Department of Defense, Mil-Std-461.

[15] United States Air Force, **Electromagnetic Compatibility Requirements for Space Systems**, Los Angeles, CA, USAF Space Division, Mil-Std-1541.

[16] United States Department of Defense. **Product Verification Requirements for Launch, Upper Stage and Space Vehicles**, El Segundo, CA, Space and Missile Systems Center, Mil-Std-1540.